

# Spectroscopy of electron-induced fluorescence in organic liquid scintillators

T. Marrodán Undagoitia<sup>1,2,a</sup>, F. von Feilitzsch<sup>1</sup>, L. Oberauer<sup>1</sup>, W. Potzel<sup>1</sup>, A. Ulrich<sup>1</sup>, J. Winter<sup>1</sup>, and M. Wurm<sup>1</sup>

<sup>1</sup> Physik-Department, Technische Universität München, James-Franck-Str., 85748 Garching, Germany

<sup>2</sup> Physik-Institut, Universität Zürich, Winterthurerstr. 190, 8050 Zürich, Switzerland

Received 21 September 2009 / Received in final form 2 December 2009

Published online 19 January 2010 – © EDP Sciences, Società Italiana di Fisica, Springer-Verlag 2010

**Abstract.** Emission spectra of several organic liquid-scintillator mixtures which are relevant for the proposed LENA detector have been measured by exciting the medium with electrons of  $\sim 10$  keV. The results are compared with spectra resulting from ultraviolet light excitation. Good agreement between spectra measured by both methods has been found.

## 1 Introduction

A new experimental method has been used to measure emission spectra of organic liquid scintillators. Commonly, such measurements are performed by exciting the medium with ultraviolet (UV) light. However, in an actual particle-astrophysics experiment charged particles excite the detection medium by depositing their kinetic energy. In this work, two methods have been used for the excitation of the scintillator: an UV-light emitter (a deuterium lamp) and an electron beam of about 10 keV energy. The experimental setups for both methods are described and the resulting spectra are compared. Electron-beam induced fluorescence has previously been used to study nitrogen fluorescence in the atmosphere [2]. Such processes are important for experiments which study cosmic-ray induced extended air showers via their fluorescence-light emission. For an optimal choice of a liquid-scintillator detection medium for a particle-physics detector, several optical parameters have to be taken into account. One of them is the scintillation emission-spectrum as it has an impact on the light propagation through the liquid. Absorption and scattering processes are wavelength dependent. In organic liquids absorption and scattering lengths increase with wavelength [1]. Additionally, the photo-cathode of the light sensors in the experiment have a wavelength-dependent sensitivity. For these reasons, it is of interest to measure the emission spectra of several scintillator candidates.

The spectroscopic measurements described in the present paper have been performed within feasibility studies for the proposed LENA (Low Energy Neutrino Astronomy) detector [3–5]. LENA is a large-volume (50 kt) observatory based on the liquid-scintillator technology. It aims

at the investigation of a variety of topics in astrophysics, geophysics and particle physics. The current detector design foresees a cylindrical shape of 100 m height and 30 m diameter placed in vertical position. Light produced in the central axis of the detector has to reach the photo-sensors which are placed at the walls of the detector. Therefore, an attenuation length of at least 10 m is required [4]. For this detector, the scintillation emission spectrum of the medium plays a major role as high transparency is necessary.

## 2 Scintillation processes

An organic liquid scintillator usually consists of a solvent medium and one or more wavelength-shifters. The kinetic energy of charged particles crossing the medium is deposited mainly in the solvent molecules and excites the electrons (in particular the  $\pi$ -electrons) of benzene-ring structures of the solvent. The  $\pi$ -electrons are delocalized and only weakly bonded. The excitation energy is rapidly transferred to the solute, usually by dipole-dipole interaction [6,7]. The efficiency of this transfer depends on the overlap of the emission spectrum of the solvent and the absorption spectrum of the solute. The de-excitation of the  $\pi$ -electron in the solute molecule leads to the emission of observable light originating from the transition between the first excited spin-singlet state and one of the vibrational levels of the ground state. A typical emission spectrum of such materials is a band of 50–100 nm width resulting from overlapping peaks. The relative intensities of the transitions to the different vibrational levels are given by the Franck-Condon factors [8,9]. Depending on the interaction of the solvent with the solute, the spectra might be broadened and/or slightly shifted in wavelength.

<sup>a</sup> e-mail: marrodan@physik.uzh.ch

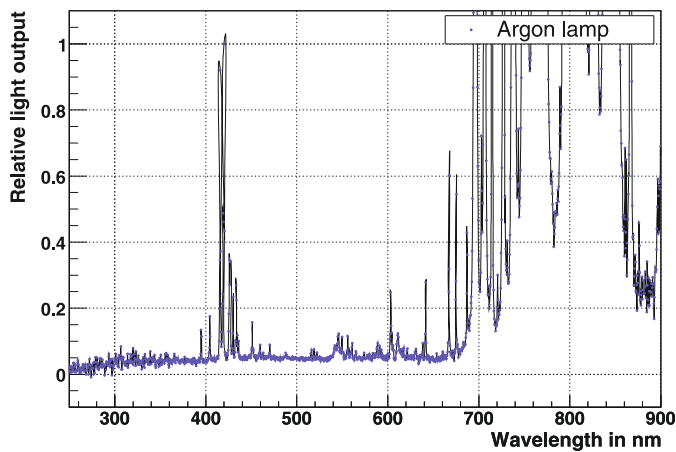


Fig. 1. (Color online) Measured spectrum of the argon lamp.

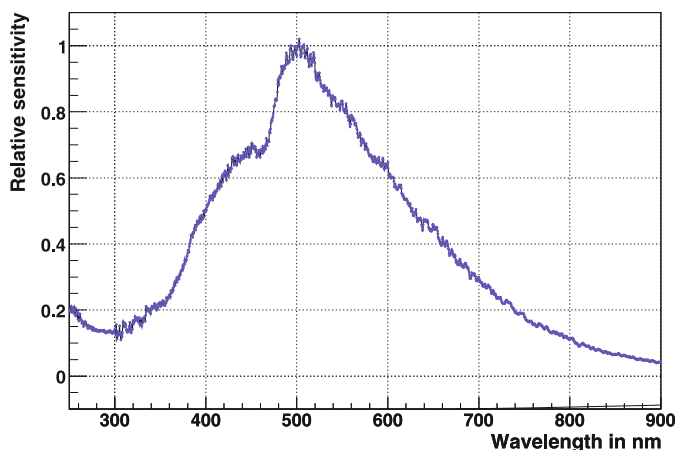


Fig. 2. (Color online) Measured response of the spectrometer at different wavelengths. The detector is most sensitive at 500 nm, while e.g. at 300 nm the efficiency drops to  $\sim 15\%$  of the maximum.

### 3 The spectrometer

The spectrometer used is of the type Ocean Optics HR2000CG-UV-NIR which is a medium-resolution miniature device [10]. It covers a wavelength range from 200 to 1100 nm with a measured resolution of 0.53 nm (full width at half maximum). The light is introduced into the spectrometer via a quartz light-guide (600  $\mu\text{m}$  in diameter). The module utilizes a 5  $\mu\text{m}$  entrance slit. Inside the spectrometer, the light is dispersed by a blaze grating which has a groove-spacing density of 300 lines/mm. The light is finally recorded by a Sony ILX511 linear CCD (charge-coupled device) array. Higher diffraction orders of the grating are blocked by edge filters. For the readout of the detector, the CCD data is extracted by a USB cable which connects the spectrometer to a computer. The output data can be analyzed offline with a custom-made program, e.g. with ROOT [11].

The spectrometer has to be calibrated in energy and the spectra have to be corrected for the intensity response at different wavelengths. For the calibration of the wavelength, a low-pressure discharge argon-lamp was used. Figure 1 shows the measured spectrum. The lines correspond to transitions of excited states of Ar atoms. The positions of distinct lines in the spectrum are tabulated. Several lines between  $\sim 350$  and 650 nm were used. The calibration showed a shift of the argon spectrum by  $1.22 \pm 0.04$  nm to higher values of the wavelength. This shift has been corrected for in the data analysis.

The wavelength dependence of the sensitivity was measured using a calibrated halogen lamp (LOT-Oriel [12]). The lamp has a known spectral emission when it is powered with 6.60 A (16.1 V) and the spectrum is measured at 70 cm distance. The spectrometer was placed at this distance and the measured spectrum was compared to the one given by the manufacturer of the halogen lamp. In Figure 2, the relative spectral response of the spectrometer is shown.

### 4 Experimental setups

Spectra were recorded by exciting the scintillator with an UV-light source, a deuterium lamp. The lamp is a low-pressure gas-discharge light source. The optical output-window of the lamp is made of magnesium fluoride in order to prevent UV-light absorption. The light emitted by the lamp was collimated and focused onto the scintillator sample by a quartz lens. Figure 3 shows a schematic drawing of the setup. The container for the scintillator sample was made out of black PTFE (polytetrafluoroethylene) material which is known not to react with liquid scintillators. The black color was chosen to suppress light reflexions. The container is a cylinder with an inner diameter of 2.5 cm and 1.0 cm length with 2 mm thick quartz windows to ensure homogeneous transmission for wavelengths down to approximately 160 nm.

The collecting optics was optimized for maximum light intensity. A quartz lens in front of the lamp was used to concentrate the UV-light at the surface of the scintillator. The UV-light is absorbed in the first  $\mu\text{m}$  to mm of the liquid. Therefore, the emission takes place also in the foremost layer of the scintillator sample. For each measurement, a light guide was used to collect the emitted light and to pass it into the spectrometer's entrance slit. Looking at the emitted light from the same side where the deuterium lamp illuminates the sample ensures that propagation effects are almost negligible as the emission takes place in the first few molecular planes.

Next, spectra of the scintillator mixtures were recorded after energy deposition of charged particles. The radiation source used for these measurements was a compact ( $\sim 20$  cm long) low-energy electron-beam device which is described in detail in [13–15]. This device is housed in a glass-metal chamber which is kept at a vacuum of  $5 \times 10^{-7}$  hPa. As indicated in Figure 4, a heated filament is used to produce the electrons. Applying a DC voltage of 10–20 kV, the electrons are accelerated towards the exit

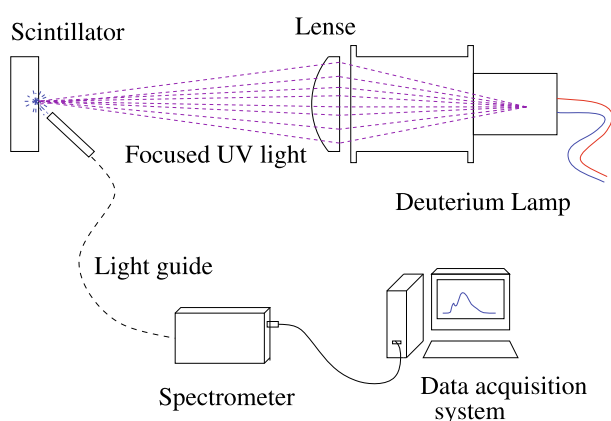


**Fig. 3.** (Color online) Setup of the spectral measurement of liquid scintillators when exciting the sample with UV-light of a deuterium lamp.

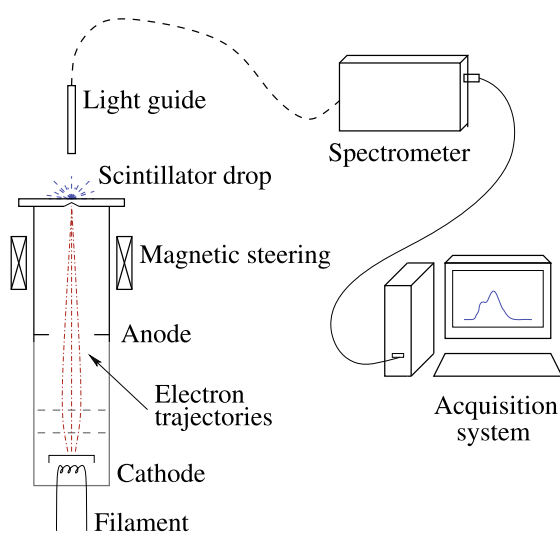


**Fig. 4.** (Color online) Setup for the spectral measurements of liquid scintillators when exciting the sample with  $\sim 10$  keV electrons.

window. Magnetic steering is used to guide the beam in the  $x$ - and  $y$ -directions, perpendicular to the electron trajectories. On the other end of the device, an exit window is realized as a  $300\ \mu\text{m}$  thick silicon wafer with an area of  $0.7 \times 0.7\ \text{mm}^2$  and a  $300\ \text{nm}$  thin foil in the center. The foil is made of  $\text{Si}_3\text{N}_4$  with an additional  $\text{SiO}_2$  layer to reduce its internal mechanical stress. The energy loss in the membrane depends on the electron energy:  $\sim 8\%$  at  $20\ \text{keV}$ ,  $\sim 15\%$  at  $15\ \text{keV}$  and  $\sim 40\%$  at  $10\ \text{keV}$  [14,16].

Figure 4 shows a schematic drawing of the experimental setup. The electron source was placed in a vertical position leading to electrons exiting in upward direction. To observe the scintillation light, a drop of the liquid sample was deposited on top of the  $\text{Si}_3\text{N}_4$  window. The drop covered a surface of about  $5\ \text{mm} \times 5\ \text{mm}$  and was about  $1\ \text{mm}$  in height. Figure 5 shows a photograph of the blue-shining scintillator drop on top of the  $\text{Si}_3\text{N}_4$  window. The

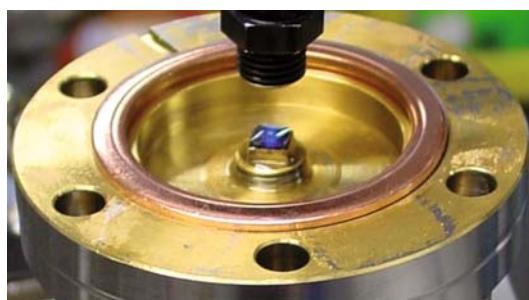


**Fig. 5.** (Color online) Photograph of the scintillator drop on top of the exit window of the electron gun.

end of the light guide was positioned about  $1\ \text{cm}$  above the window. The samples were taken from bottles with nitrogen atmosphere and the measurements were performed immediately thereafter (within the next 10 min) to minimize oxygen diffusion into the sample, i.e. to prevent a degradation of the scintillator. During the measurements, a decrease of the emitted light intensity with time was observed. Two probable explanations are favored: either the intense  $e^-$ -radiation damaged the liquid by destroying the constituent  $\sigma$ -bonds or the scintillator drop evaporated partially with time, causing a loss of scintillating material in the sample.

## 5 Results and discussion

Four samples were investigated:

- PXE with  $2\ \text{g/L}$  PPO;
- PXE with  $2\ \text{g/L}$  PPO and  $20\ \text{mg/L}$  bisMSB;
- LAB (P550 Q) with  $2\ \text{g/L}$  PPO; and
- PXE with  $2\ \text{g/L}$  PMP.

The solvents used were phenyl-*o*-xylethane (PXE) and linear-alkyl-benzene (LAB, from Petresa Company type P550 Q [17]). The solutes dissolved were 2,5-diphenyl-oxazole (PPO), 1,4-bis-(*o*-methylstyryl)-benzene (bisMSB) and 1-phenyl-3-mesityl-2-pyrazoline (PMP).

The spectra obtained by the methods described in Section 4 are shown in Figure 6. In each plot, the blue data points (open circles) represent the emission spectra obtained by electron-beam excitation after the light has propagated through the scintillator drop. The excitation was produced by  $\sim 10\ \text{keV}$  electrons. The data points obtained by UV-light excitation are also plotted (green full circles) for comparison [5]. The spectra are normalized in intensity such that the highest intensity corresponds to 1. The spectrometer was calibrated as described in Section 3. In the UV-region, the data points are more scattered; this is due to the comparatively low sensitivity of the spectrometer in this wavelength region (see Fig. 2).

Except for the PMP solute, the emission spectra show clear peaks. For example in the case of the PPO solute (upper left in Fig. 6), the peaks are approximately at  $350$ ,  $365$ ,  $380$  and  $395\ \text{nm}$ . These peaks show the energy spacing

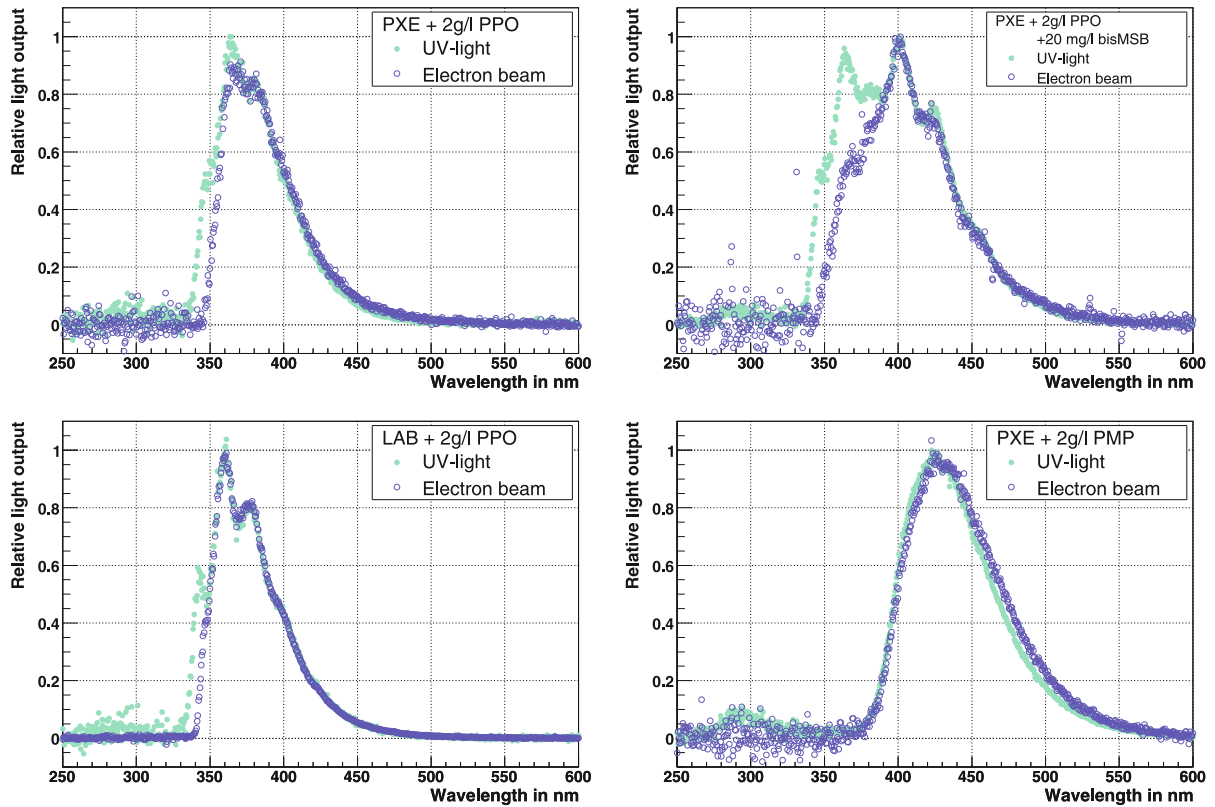


**Fig. 6.** (Color online) Spectra obtained with the electron-beam excitation method. The blue data points (open circles) represent the emission spectra of different scintillator mixtures after the light has propagated through the drop. For comparison [5], data from the UV-light excitation method is also plotted (green full circles). Samples: PXE + 2 g/L PPO, PXE + 2 g/L PPO + 20 mg/L bisMSB, LAB + 2 g/L PPO, and PXE + 2 g/L PMP. The excitation is produced by  $\sim 10$  keV electrons.

between the first singlet excited state,  $S_1$ , and the different vibrational levels of the ground state of the solute,  $S_{0i}$ . The relative intensities of the vibrational lines in the spectrum of PPO are compatible with the literature results [18]. The energy spacing between the ground state and the first excited triplet state is in general smaller, i.e. at longer wavelengths, than that of the first excited singlet state. As no significant contribution appears above  $\sim 500$  nm, it can be concluded that there is no evidence for phosphorescence in the measured spectra. PMP displays a broad and less structured fluorescence spectrum which has also been reported in the literature [19].

For mixtures containing the solute PPO and the solvents PXE and LAB, the shapes of the spectra above 375 nm obtained by electron excitation are almost identical to those measured by observing the UV-illuminated front layer of the scintillator. The main difference arises from the absorption at short wavelengths due to the transmission through the scintillator drop. Short wavelengths are rapidly absorbed within the first mm of the drop in the electron-beam experiment.

The spectra of PXE with PMP differ only in the region from  $\sim 450$  to  $\sim 550$  nm for the two excitation methods studied. The UV-induced intensity is maximally 5% lower in this regime. This observation could be an indication of different molecular processes for the two studied excitation

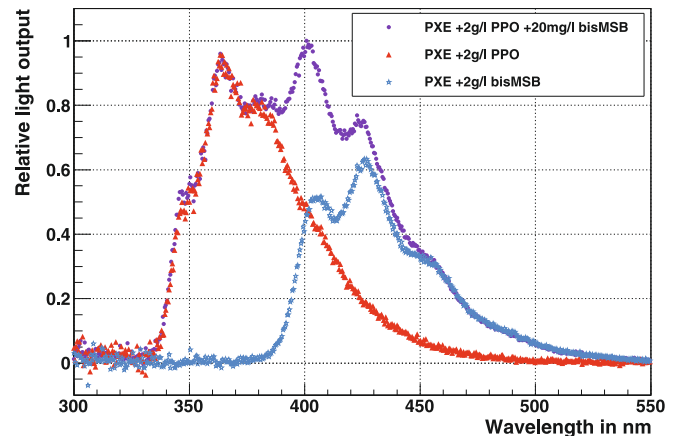


**Fig. 7.** (Color online) Zoom into the spectra of 2 g/L PPO and 20 mg/L bisMSB (violet points), 2 g/L PPO (red triangles) and 2 g/L bisMSB (blue stars). All individual mixtures are dissolved in the solvent PXE and excited by UV light. The three-component scintillator (violet points) can be seen to be the sum of the spectra of both solutes.

methods. However, the effect is not significant enough to extract relevant conclusions.

The spectrum of the mixture of PXE with 2 g/L PPO and 20 mg/L bisMSB (upper right in Fig. 6) shows very

interesting features. To determine the origin of the various peaks, in Figure 7 the spectra of PXE with 2 g/L PPO and 20 mg/L bisMSB (violet points), PXE with 2 g/L PPO (red triangles) and PXE with 2 g/L bisMSB (blue stars) are displayed together for the wavelength region between 300 nm and 550 nm. These spectra have been obtained by exciting the scintillators with UV-light. Figure 7 clearly shows that the three-component spectrum (violet points) results as the sum of the PPO and bisMSB spectra. Although the concentration of bisMSB is only 20 mg/L, its contribution to the sum spectrum is highly significant.

The features of the spectrum in Figure 6 (upper right) can be explained by the following processes: when the UV-light from the deuterium lamp enters the scintillator, mostly PXE molecules are excited. The energy is rapidly transferred to PPO, mainly by nonradiative processes. Part of the energy in the PPO molecule is transferred further on to bisMSB molecules in the same manner. As the concentration of bisMSB is low (in the order of several mg/L), some of the PPO molecules find no bisMSB partners. As a consequence, the light is partly emitted by the PPO molecules themselves. The spectrum is therefore an overlap of the PPO and the bisMSB spectra. Although the concentration of bisMSB is low, the contribution of bisMSB to the sum spectrum is  $\sim 40\%$ . This illustrates the efficient energy transfer from PPO to bisMSB. Above 400 nm, the two spectra obtained by UV-light or electron-beam excitation (see Fig. 6) are practically identical. Around 350 nm, the absorption at short wavelengths can be observed in the spectrum with electron excitation as in the previous cases. The most interesting region is between 350 and 400 nm, where the contribution of PPO to the spectrum by electron excitation is strongly reduced compared to the spectrum obtained by UV-excitation. This can be explained by the fact, that the light has to propagate through the scintillator drop (about a mm). Within this propagation distance, bisMSB very efficiently absorbs the light emitted by PPO. Consequently, the part of the spectrum due to the bisMSB emission is increased compared to that due to PPO.

Considering the differences in the spectra of PPO in the solvents PXE and LAB (the two spectra on the left side of Fig. 6), a shift of 5–10 nm to longer wavelengths of all the PPO vibrational peaks for the PXE solvent is observed. Furthermore, the resolution of the vibrational levels differs: the peaks in the mixture with LAB are better resolved. These effects can be explained by considering the structure of the solvent molecules. PXE consists of two benzene rings and several  $\text{CH}_3$  groups while LAB has only one benzene ring and a long hydrocarbon-chain. The solvent molecules surrounding the benzene rings of PPO produce a mean effective potential which influences the space available to the orbitals of the  $\pi$ -bonds of the solute molecule. The solute feels this effective potential which might result in a different emission spectrum. In addition, this mean potential can change the intrinsic lifetime of the solute fluorescence [18]. For example, it has been found that the lifetime of PPO dissolved in PXE is shorter than when dissolved in LAB [20]. Similar effects have indeed

been observed and described in the literature [18]. A further consequence of this effective potential could be the wavelength difference of the peak emission of the solvents PXE and LAB, namely at 290 and 283 nm, respectively, reported in [21,22]. In some of the spectra, the emission of the solvent can be seen around 300 nm. The contribution is however, very small because the solute very effectively gets the energy transferred from the solvent to the solute.

## 6 Conclusions

Spectroscopy on organic liquid scintillators relevant for the proposed LENA detector has been performed. The scintillators have been excited using a new method: a table-top electron beam source. For comparison, spectra are shown where the excitation occurs by UV-light. Apart from absorption effects due to the propagation of light through a thin layer of scintillator, both excitation methods return comparable results for the measured samples. A precise knowledge of the emission spectra of liquid scintillators is of great interest for the proposed LENA detector as the propagation of the light (absorption and scattering processes) is wavelength dependent.

By studying the mixture of the solvent PXE with 2 g/L PPO and a low concentration of bisMSB (20 mg/L) it has been found that the energy transfer between both wavelength-shifters happens very efficiently already within short distances ( $< \text{mm}$ ). The electron-beam setup can be used in the future to measure emission spectra of further organic scintillators.

We want to thank A. Morozov for his help during the measurements. This work has been supported by funds of the Maier-Leibnitz-Laboratorium (Munich), the Deutsche Forschungsgemeinschaft (DFG) (transregio TR27: Neutrinos and Beyond) and the Munich Cluster of Excellence (Origin and Structure of the Universe).

## References

1. G. Alimonti et al. (Borexino), Nucl. Instrum. Meth. A **440**, 360 (2000)
2. M. Ave et al. (AIRFLY Collaboration), Astropart. Phys. **28**, 41 (2007)
3. T. Marrodán Undagoitia et al., Prog. Part. Nucl. Phys. **57**, 283 (2006)
4. T. Marrodán Undagoitia et al., Phys. Rev. D **72**, 075014 (2005)
5. T. Marrodán Undagoitia, Ph.D. thesis, Technische Universität München, Garching, Germany, 2008, <http://mediatum2.ub.tum.de/doc/667813/667813.pdf>
6. J.B. Birks, *The Theory and Practice of Scintillation Counting* (Pergamon Press, London, 1964)
7. C. Buck, Ph.D. thesis, Ruperto-Carola Universität, Heidelberg, Germany, 2004
8. J. Franck, E.G. Dymond, Trans. Faraday Soc. **21**, 536 (1926)
9. E. Condon, Phys. Rev. **28**, 1182 (1926)

10. Ocean Optics (2007), <http://www.oceanoptics.com/>
11. F. Rademakers, R. Brun, Linux Journal **51** (1998)
12. LOT-Oriel, [www.lot-oriel.com/](http://www.lot-oriel.com/)
13. J. Wieser et al., Rev. Sci. Instrum. **68**, 3 (1997)
14. A. Morozov et al., Eur. Phys. J. D **33**, 207 (2005)
15. A. Ulrich et al., Eur. Phys. J. Appl. Phys. **47**, 22815 (2009)
16. A. Morozov et al., Eur. Phys. J. D **48**, 383 (2007)
17. Petresa Canada Inc. (PCI), 5250 Bécancour Blvd., Québec, G9H 3X3 Canada
18. I.B. Berlman, *Handbook of fluorescence spectra of aromatic molecules* (Academic Press, New York and London, 1971)
19. H. Guesten, P. Schuster, W. Seitz, AIP Conf. Proc. **82**, 459 (1978)
20. T. Marrodán Undagoitia, Rev. Sci. Instrum. **80**, 043301 (2009)
21. H.O. Back et al., Nucl. Instrum. Meth. A **585**, 48 (2008)
22. C. Buck, private communication (2007)